Density of topological constraints as a metric for predicting glass hardness

Zheng, Qiuju; Yue, Yuanzheng; Mauro, John C.

Published in:
Applied Physics Letters

DOI (link to publication from Publisher):
10.1063/1.4991971

Publication date:
2017

Document Version
Publisher's PDF, also known as Version of record

Applied Physics Letters

Density of topological constraints as a metric for predicting glass hardness

Cite as: Appl. Phys. Lett. **111**, 011907 (2017); https://doi.org/10.1063/1.4991971
Submitted: 17 April 2017 . Accepted: 23 June 2017 . Published Online: 07 July 2017

Qiuju Zheng, Yuanzheng Yue, and John C. Mauro

Density of topological constraints as a metric for predicting glass hardness

Qiuju Zheng,[1] Yuanzheng Yue,[1,2,a)] and John C. Mauro[1,3,4,a)]
[1]School of Materials Science and Engineering, Qilu University of Technology, 250353 Jinan, China
[2]Department of Chemistry and Bioscience, Aalborg University, DK-9220 Aalborg, Denmark
[3]Science and Technology Division, Corning Incorporated, Corning, New York 14831, USA
[4]Department of Materials Science and Engineering, The Pennsylvania State University, University Park, Pennsylvania 16801-7003, USA

(Received 17 April 2017; accepted 23 June 2017; published online 7 July 2017)

Topological constraint theory has previously been applied to predict the composition dependence of glass hardness for a variety of different composition families. Some recent findings have cast doubt on the correlation between glass hardness and the number of rigid constraints per atom in silicate glasses. In this letter, we revisit the prediction of hardness for borosilicate and phosphosilicate glasses using four different types of constraint counting approaches: total number of constraints per atom, angular constraints per atom, total constraint density, and angular constraint density. We find that the counting approaches using total constraint density or angular constraint density give an improved prediction of glass hardness. We therefore conclude that glass hardness is governed by the density of rigid constraints under an indenter, rather than by the number of rigid constraints per atom. *Published by AIP Publishing*. [http://dx.doi.org/10.1063/1.4991971]

Glass hardness is of great importance for developing high-tech glass devices, e.g., scratch-resistant glass covers for smart phones and touch sensitive electronic devices.[1–7] Hardness (H_V) is defined as the applied load divided by the projected area of the deformed region of the material and is a measure of the ability of a material to resist permanent deformation under a load. Due to the non-crystalline structure and the nonequilibrium nature of glass, direct prediction of glass hardness from first principles has proven challenging.[8] While hardness is often correlated with elastic moduli—since elastic deformation is an important part of the indentation process—this correlation is not universal.[9,10]

Topological constraint theory has proven to be a powerful tool for predicting the composition dependence of several glass properties.[11–17] This theory treats the atomic structure of glass as a network of rigid constraints, where the macroscopic properties of a glass are related to the composition, temperature, and pressure dependence of these constraints. Smedskjaer, Mauro, and Yue established a constraint counting model where the hardness of borate glasses can be predicted within experimental uncertainty.[18,19] According to this model, a certain critical number of constraints (n_{crit}) must be present for the material to display mechanical resistance, i.e., for hardness to become nonzero in three dimensions. When the average number of atomic constraints, n, is less than this critical value ($n < n_{crit}$), the mechanical response is liquid-like, i.e., there is no resistance to an incoming indenter and hence no measurable hardness. When $n > n_{crit}$, there are enough constraints to make a rigid network that produces a solid-like mechanical response. A value of $n = 2$ gives a network that is rigid along one dimension, such as in selenium glass, which consists of one-dimensional rods with rigid radial bonds and intra-chain bond angles. A value of $n = 3$ indicates a network that is rigid in three dimensions, such as silica, which consists of a fully connected network of corner-sharing tetrahedra. A network must be rigid in at least two dimensions to be mechanically resistant. This corresponds to $n_{crit} = 2.5$ (Ref. 18) and represents a network that is exactly rigid in two dimensions of the three-dimensional space, such as in planar sheets of graphene. The hardness of a glass is therefore proportional to the number of additional constraints in excess of n_{crit}[18]

$$H_V(x) = \left(\frac{dH_V}{dn}\right)[n(x) - n_{crit}] = \left(\frac{dH_V}{dn}\right)[n(x) - 2.5], \quad (1)$$

where x represents the glass composition as a variable and $n(x)$ is the number of rigid constraints per network-forming atom at the temperature of the hardness measurement as a function of chemical composition (x). The rigidity of the constraints depends on the temperature of the system. At high temperatures, the network is flexible since there is enough thermal energy to overcome the bond constraints. As the temperature decreases, additional constraints become rigid due to the reduced thermal energy. Since the hardness of a glass is typically measured at room temperature, the number of rigid constraints per atom should also be calculated at room temperature. In Eq. (1), dH_V/dn is the load-dependent proportionality, which is determined empirically, i.e., the slope of a linear fit of H_V as a function of n. It should be mentioned that H_V must be a non-negative quantity. In this work, H_V refers to the hardness measured at room temperature. This model was first applied to a series of soda lime borate glasses, with excellent agreement between modeled and measured values of hardness. However, the model performed less accurately for predicting the hardness of two silicate glass systems, viz., borosilicate and phosphosilicate glasses.[20,21]

Some recent findings have offered alternative approaches for correlating the number of rigid constraints to the hardness of the glass. When predicting the hardness of a series of calcium aluminosilicate (CAS) glasses, Lamberson found poor fitting quality using Eq. (1) (Ref. 22) and proposed a correlation of hardness with constraint density, i.e., the number of

a)Author to whom correspondence should be addressed: yy@bio.aau.dk and mauroj@corning.com

rigid constraints per unit volume rather than per atom, giving an improved fit quality for her glasses with $[SiO_2] < 85$ mol. %. Bauchy *et al.* proposed another approach for calculating hardness based on counting the number of angular constraints per atom, neglecting the contribution of the two-body radial constraints.[23] Radial constraints are the two-body constraints which correspond to the rigid bond lengths between pairs of atoms, and angular constraints are the three-body constraints which correspond to rigid bond angles.[13] According to their argument, angular and radial constraints have different contributions to the resistance of the glass to different types of deformation. Bauchy *et al.* and Jiang *et al.* argued that hardness is related more to the resistance to shear flow,[23,24] and thus hardness should depend predominantly on the number of angular constraints. They applied this model to a complex material, calcium-silicate-hydrate (CSH), the binding phase of concrete, which contains both non-crystalline and crystalline phases, and showed good linear correlation between hardness and the number of angular constraints per atom. Based on these results, they argued that hardness is dominated by the weak atomic constraints, and topological models of hardness should consider angular constraints only instead of the total number of rigid constraints.

In this work, we analyze the room temperature hardness data of previously published borosilicate and phosphosilicate systems to compare these various constraint counting approaches when modeling glass hardness with topological constraint theory. We calculate hardness of the two glass series using four different constraint counting approaches: total number of constraints per atom, angular constraints per atom, constraint density, and angular constraint density. By comparing the fitting ability of the different counting approaches, we find that the counting approaches using total constraint density or angular constraint density yield the most accurate fit to hardness data for silicate glasses. Therefore, the total constraint density or angular constraint density can be used as a metric for predicting silicate glass hardness.

In this study, the borosilicate and phosphosilicate glasses were prepared using the melt-quenching method. The nominal molar compositions of the borosilicate glasses are $(0.75–y)SiO_2{\cdot}yB_2O_3{\cdot}0.15Na_2O{\cdot}0.10CaO$, where $y = 0$, 0.06, 0.12, 0.24, 0.375, 0.51, 0.63, and 0.75. The molar compositions of the phosphosilicate glasses are $0.3Na_2O{\cdot}0.7[zSiO_2 \cdot (1-z)P_2O_5]$, with $z = 0$, 0.14, 0.29, 0.43, 0.54, 0.89, and 1.00. The compositions of all glasses have been analyzed using wet chemistry methods, and the measured compositions are used as input in the models. The densities of all of the glass samples were determined using Archimedes principle. The Vickers microhardness (H_V) values of the glasses were measured using a Duramin 5 indenter (Struers A/S) in air at room temperature. For the borosilicate glasses, the indentations were performed at a load of 0.25 N for a duration of 5 s. For the phosphosilicate glasses, the indentations were performed at a load of 0.49 N for duration of 15 s. The hardness of each sample was measured at 30 widely separated locations. The details of sample preparation and hardness measurements have been described elsewhere.[20,21]

For the modeling of glass hardness, we first calculate the total number of constraints per atom and the angular constraints per atom for the two glass systems, and then apply Eq. (1) to calculate hardness. Figure 1 in Ref. 13 illustrates the counting of radial and angular constraints. The detailed constraints calculations for the borosilicate and phosphosilicate glasses have been described in Refs. 20 and 21, respectively. When using the total number of constraints per atom, n_{crit} is set equal to 2.5 as described earlier; however, when using the angular constraints per atom, n_{crit} is lower and varies with composition since the radial constraints are not included as part of the calculation.

The density and molar mass data are used to convert the total number of constraints per atom and the angular constraints per atom to total constraint density and angular constraint density, respectively, using the following equation:

$$n'(x) = \frac{n(x) \cdot \rho(x) \cdot N_A}{M(x)}, \tag{2}$$

where $n'(x)$ is the constraint density, $n(x)$ is the number of constraints per atom, $\rho(x)$ is the glass density, N_A is Avogadro's number, and $M(x)$ is the molar mass. When considering $n(x)$ as the number of angular constraints per atom, $n'(x)$ refers to the angular constraint density.

Each glass network has its own set of bond constraints, which are a function of the underlying glass chemistry.[25–27] These constraints may include two-body radial constraints, three-body angular constraints, and, for some systems, constraints associated with modifier clustering. Here, we consider both the total number of constraints for a given system, as well as the radial and angular constraints separately, for the borosilicate and phosphosilicate glasses. As shown in Figs. 1(a) and 2(a), the number of radial constraints per atom for the two glass systems is comparable, and there is little variation in the number of radial constraints as a function of composition within each glass family. However, the number of angular constraints per atom differs significantly between the two glass systems, and it shows large compositional dependence within each glass family. Hence, it is clear that the angular constraints per atom play the dominant role in governing the evolution of the total number of constraints per atom in each system. A similar trend is found for the composition dependence of total constraint density, but with more pronounced variations [Figs. 1(b) and 2(b)]. The phosphosilicate glasses are slightly underconstrained, having a total number of constraints fewer than the number of degrees of freedom, while the borosilicate glasses are overconstrained at room temperature.

When we use total constraint density, the glass hardness is calculated using the following variation of Eq. (1):

$$H_V(x) = \left(\frac{dH_V}{dn}\right) n'(x), \tag{3}$$

where $n'(x)$ refers to total constraint density. We propose that hardness is directly proportional to the magnitude of the total constraint density. If there is zero total constraint density, then the hardness should be zero. There is only one fitting parameter in this model, viz., the constant of proportionality. As displayed in Fig. 3(a), good agreement is found between the modeled and measured values of hardness for both the borosilicate glasses and phosphosilicate glasses. These results indicate that the hardness converges at zero when the total constraint density is zero, which gives a

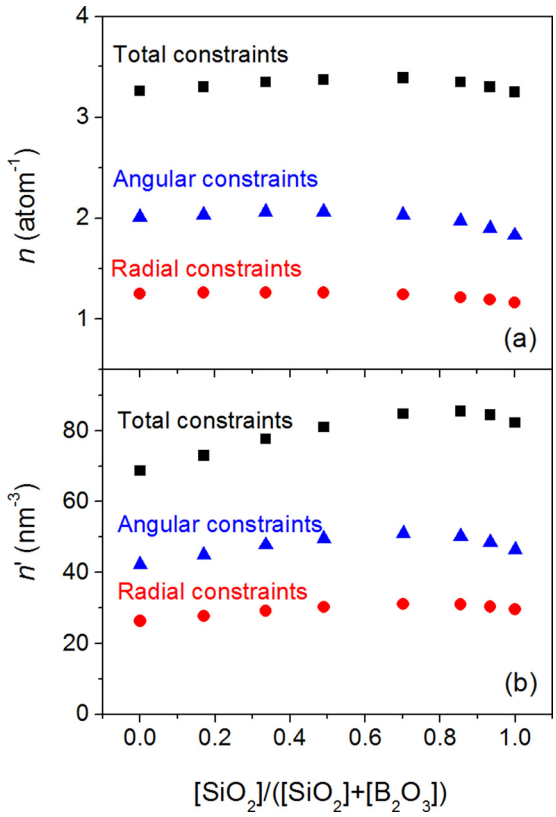

FIG. 1. (a) The number of radial, angular, and total constraints per atom, n (atom^{-1}), as a function of composition for the borosilicate glasses, (0.75-y) SiO_2·yB_2O_3·0.15Na_2O·0.10CaO, with $y = 0$ to 0.75. (b) The composition dependence of constraint density, n'(nm^{-3}).

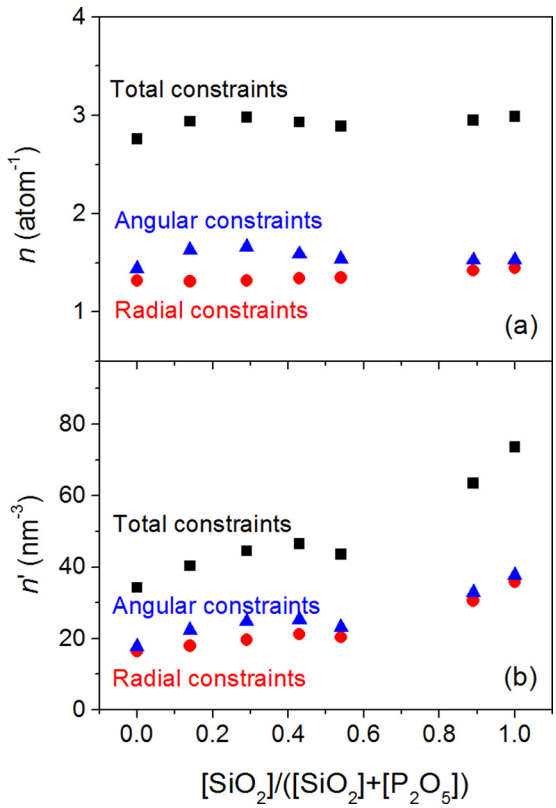

FIG. 2. (a) The number of radial, angular, and total constraints per atom, n (atom^{-1}), as a function of composition for the phosphosilicate glasses, 0.3Na_2O·0.7[$z$$SiO_2$ · (1 − z)P_2O_5], with $z = 0$ to 1. (b) The composition dependence of constraint density, n' (nm^{-3}).

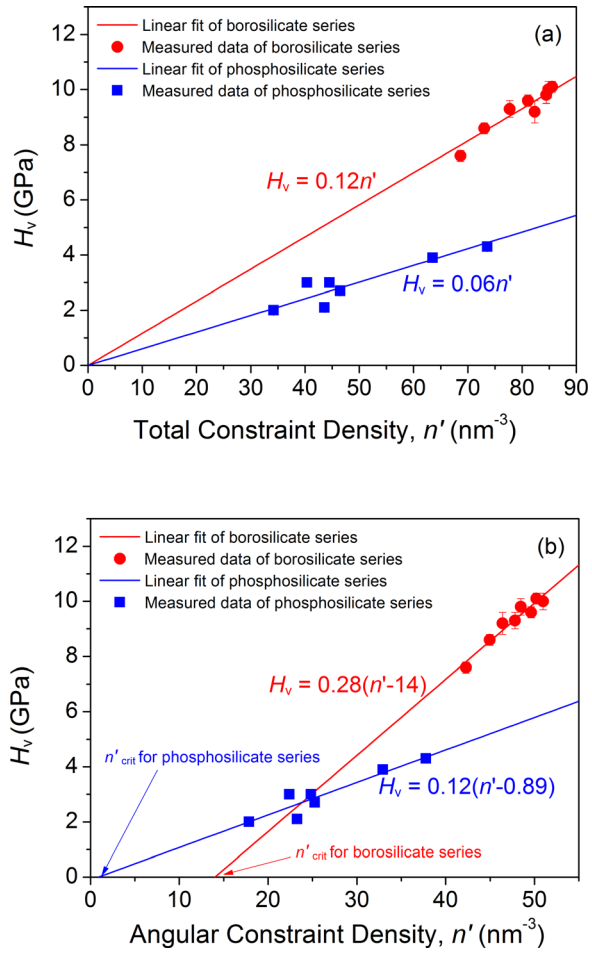

FIG. 3. Measured and modeled hardness as a function of (a) total constraint density and (b) angular constraint density, (n') (nm^{-3}) for the borosilicate glasses (0.75-y)SiO_2·yB_2O_3·0.15Na_2O·0.10CaO with $y = 0$–0.75 and phosphosilicate glasses 0.3Na_2O·0.7[$z$$SiO_2$ · (1 − z)P_2O_5], with z = 0–1.00. The solid line represents the linear fit of the measured data to Eq. (3).

common intercept for these two systems. This significantly simplifies the process for modeling of glass hardness and may perhaps indicate a universal law of glass hardness.

With angular constraint density, the glass hardness is calculated using the following variation of Eq. (1):

$$H_V(x) = \left(\frac{dH_V}{dn}\right)\left[n'(x) - n'_{crit}\right], \tag{4}$$

where $n'(x)$ refers to angular constraint density and the zero hardness intercept, n'_{crit}, is treated as an empirical fitting parameter rather than assuming a particular value as in Eq. (1). Figure 3(b) shows the modeled hardness using Eq. (4) as a function of angular constraint density, where good agreement is seen between the modeled and measured hardness values. While in Eqs. (1) and (3), the zero hardness intercepts, n_{crit}, are a universal values, in Eq. (4), the zero hardness intercept n'_{crit} is not a fixed value, since the proportion of angular constraints varies with different glass systems. When considering the angular constraint density, the value of n'_{crit} in Eq. (4) should correspond to a system with n_{crit} = 2.5 in Eq. (1), corresponding to a hardness of zero. Hence, n'_{crit} can be viewed as the critical value of angular constraint density to achieve nonzero hardness, and depends on the

number of different types of bonds, their strengths, and the molar volume of the glass. Then, the hardness values of the glasses are linearly proportional to the number of additional angular constraint density in excess of n'_{crit}. As indicated in Fig. 3(b), n'_{crit} varies when using angular constraint density for the borosilicate glasses and phosphosilicate glasses.

Figure 4 shows a comparison of the experimental hardness data for the borosilicate glasses with the four different types of constraint models considered earlier. The predictive ability of the four hardness models can be quantified using the coefficients of determination (R^2) summarized in Table I. There is a clear improvement in fitting quality when considering the total constraint density rather than the total number of constraints per atom [Fig. 4(a)]. As displayed in Table I, the R^2 values of the model using total constraint density is much higher than that of using the total number of constraints per atom. As shown in Fig. 4(b) and Table I, the hardness model based on angular constraint density also shows very good agreement with the experimental data with the highest R^2 value, while the modeled hardness using angular constraints per atom gives poor agreement with very low R^2 value. It should be noted that the hardness prediction using angular constraint density is slightly better than that using total constraint density, with a marginally higher R^2 value. Either counting approach based on constraint density dramatically improves the fitting quality compared to using constraints per atom.

The scenario for the phosphosilicate glasses is quite similar to that of the borosilicate glasses, as depicted in Fig. 5.

TABLE I. R^2 values for the four types of fit using different counting approaches for the borosilicate and phosphosilicate glasses.

Counting approach \ Glass series	Borosilicates	Phosphosilicates
Total constraints per atom	0.424	0.549
Total constraint density	0.920	0.837
Angular constraints per atom	0.015	0.026
Angular constraint density	0.938	0.867

The predicted trends of hardness as a function of glass composition using both constraint density approaches exhibit better agreement with the measured hardness compared to either type of constraint counting on a per atom basis. It can be seen in Table I that the fitting using angular constraint density is the best with the highest R^2 values. The counting approach using total constraint density yields the second best fitting quality with slightly lower R^2 values. The fitting quality using angular constraints per atom is the worst with the lowest R^2 values.

Lamberson attempted to predict the hardness of a series of calcium aluminosilicate (CAS) glasses by topological constraint theory.[22] She found a breakdown in the correlation between hardness and total number of constraints per atom and proposed constraint density as an improved method to predict hardness. Since hardness is a measure of pressure, i.e., force per unit area, it is reasonable to infer that constraint density is the controlling factor for mechanical properties. During the indentation process, the indenter is

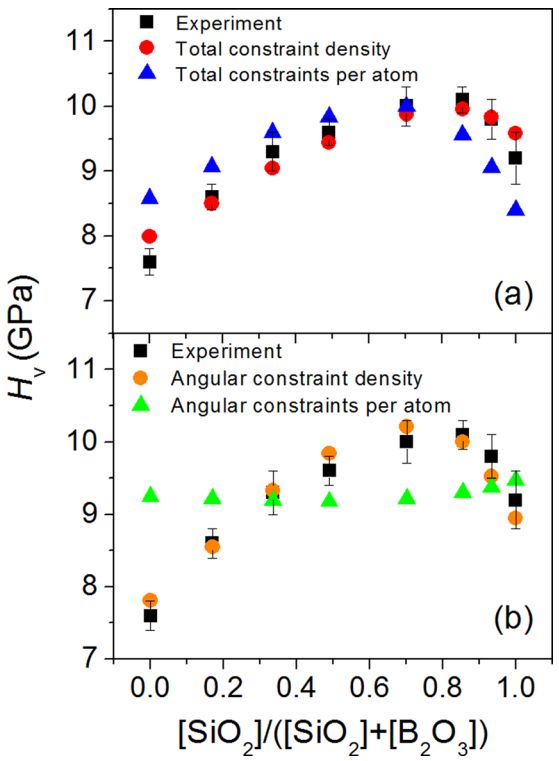

FIG. 4. Composition dependence of Vickers hardness (H_V) for the borosilicate glasses. The squares represent the experimental H_V data. (a) The circles and triangles represent the modeled H_V data using total constraint density and total constraints per atom. (b) The circles and triangles represent the modeled H_V data using angular constraint density and angular constraints per atom, respectively.

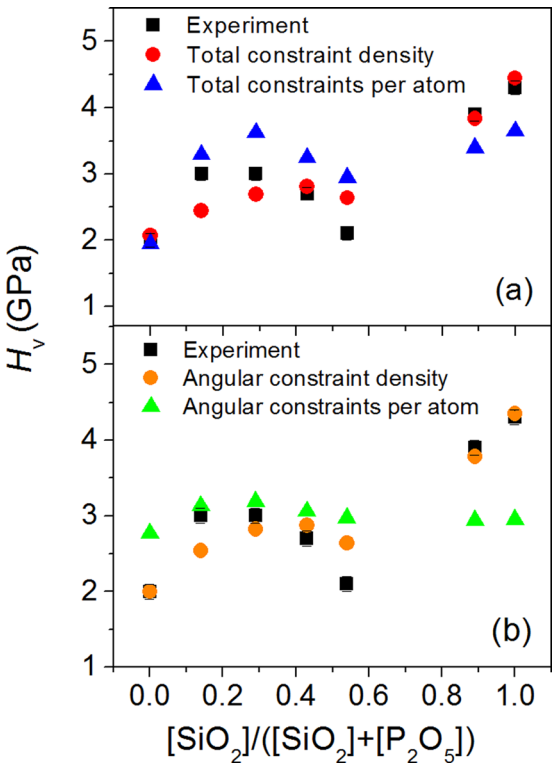

FIG. 5. Composition dependence of Vickers hardness (H_V) for the phosphosilicate glasses. The squares represent the experimental H_V data. (a) The circles and triangles represent the modeled H_V data using total constraint density and total constraints per atom. (b) The circles and triangles represent the modeled H_V data using angular constraints density and angular constraints per atom, respectively.

interacting with certain volume of the glass rather than a fixed number of atoms. Even if the number of constraints per atom is high, the resistance to deformation of a glass with a low constraint density may not necessarily be high. Therefore, constraint density plays a more dominant role for determining hardness. It should be noted that each bond constraint corresponds to a certain energy since different kind of bond has different bonding energy,[28] and thus the constraint density also represents an energy per unit volume. In other words, hardness is correlated to the energy per unit volume. Our findings for the borosilicate and phosphosilicate systems are further evidence in support of this argument, since both the total constraint density and angular constraint density approaches give better prediction of glass hardness compared to models based on number of atomic constraints.

Bauchy *et al*. have extended the topological model to calcium-silicate-hydrate (CSH), showing that hardness is dominated by angular constraints.[29,30] They proposed that the indentation process should preferably involve breaking or reformation of angular constraints, and therefore the hardness should be driven only by the weaker atomic constraints, i.e., the angular constraints. Their modeled hardness using angular constraints per atom agreed very well with the experimental data. Our results show that the composition dependence of constraints for borosilicate and phosphosilicate glasses is indeed dominated by the variation in number of angular constraints, both on a per atom and per unit volume basis. We have shown that the hardness prediction using angular constraint density is slightly better than that using total constraint density. This finding is further support that the angular constraints play a key role during the indentation process.

In summary, the best linear constraint model of silicate glass hardness is obtained based on the density of angular constraints. Total constraint density works nearly as well, since the composition dependence of the total constraints is dominated by the variation in the angular constraints. The total constraint density model of Eq. (3) has the additional advantage of being a simpler model with only one fitting parameter. Based on our findings and combining the approaches of Lamberson and Bauchy, we propose that the density of rigid total constraints or rigid angular constraints should be used as a metric for predicting silicate glass hardness. Additional research should be conducted to study the dominant drivers of hardness for other families of glass chemistry and determine whether Eq. (3) is indeed a universal model for glass hardness.

We are grateful for many valuable discussions with Morten Smedksjaer and Christian Hermansen (Aalborg University), Mathieu Bauchy (UCLA), Lisa Lamberson (Corning Incorporated), and Shefford Baker (Cornell University).

[1]H. Li and R. C. Bradt, J. Non-Cryst. Solids **146**, 197 (1992).
[2]M. Yamane and J. D. Mackenzie, J. Non-Cryst. Solids **15**, 153 (1974).
[3]M. Bertoldi and V. M. Sglavo, J. Non-Cryst. Solids **344**, 51 (2004).
[4]A. Simunek and J. Vackar, Phys. Rev. Lett. **96**, 085501 (2006).
[5]A. Faivre, F. Despetis, F. Guillaume, and P. Solignac, J. Am. Ceram. Soc. **93**, 2986 (2010).
[6]J. Kjeldsen, Ph.D. thesis, Aalborg University, Aalborg, Denmark, 2014.
[7]K. Suzuki, Y. Benino, T. Fujiwara, and T. Komatsu, J. Am. Ceram. Soc. **85**, 3102 (2002).
[8]L. Wondraczek and J. C. Mauro, J. Eur. Ceram. Soc. **29**, 1227 (2009).
[9]Y. T. Cheng and C. M. Cheng, Appl. Phys. Lett. **73**, 614 (1998).
[10]H. Yoshino and M. Mézard, Phys. Rev. Lett. **105**, 015504 (2010).
[11]P. K. Gupta and J. C. Mauro, J. Chem. Phys. **130**, 094503 (2009).
[12]J. C. Mauro, P. K. Gupta, and R. J. Loucks, J. Chem. Phys. **130**, 234503 (2009).
[13]J. C. Mauro, Am. Ceram. Soc. Bull. **90**, 31 (2011).
[14]Q. J. Zheng and J. C. Mauro, J. Am. Ceram. Soc. **100**, 6 (2017).
[15]M. Micoulaut and Y. Z. Yue, MRS Bull. **42**, 18 (2017).
[16]D. R. Swiler, A. K. Varshneya, and R. M. Callahan, J. Non-Cryst. Solids **125**, 250 (1990).
[17]H. D. Zeng, Q. Jiang, Z. Liu, X. Li, J. Ren, G. R. Chen, F. Liu, and S. Peng, J. Phys. Chem. B **118**, 5177 (2014).
[18]M. M. Smedskjaer, J. C. Mauro, and Y. Z. Yue, Phys. Rev. Lett. **105**, 115503 (2010).
[19]M. M. Smedskjaer, Front. Mater. **1**, 23 (2014).
[20]M. M. Smedskjaer, J. C. Mauro, R. E. Youngman, C. L. Hogue, M. Potuzak, and Y. Z. Yue, J. Phys. Chem. B **115**, 12930 (2011).
[21]C. Hermansen, X. J. Guo, R. E. Youngman, J. C. Mauro, M. M. Smedskjaer, and Y. Z. Yue, J. Chem. Phys. **143**, 064510 (2015).
[22]L. A. Lamberson, Ph.D. thesis, Cornell University, Ithaca, New York, U.S.A., 2016.
[23]M. Bauchy, M. J. A. Qomi, C. Bichara, F. Ulm, and R. J. M. Pellenq, Phys. Rev. Lett. **114**, 125502 (2015).
[24]X. Jiang, J. Zhao, and X. Jiang, Comput. Mater. Sci. **50**, 2287 (2011).
[25]J. C. Phillips, J. Non-Cryst. Solids **34**, 153 (1979).
[26]J. C. Phillips and M. F. Thorpe, Solid State Commun. **53**, 699 (1985).
[27]C. Hermansen, J. C. Mauro, and Y. Z. Yue, J. Chem. Phys. **140**, 154501 (2014).
[28]C. Hermansen, B. P. Rodrigues, L. Wondraczek, and Y. Z. Yue, J. Chem. Phys. **141**, 244502 (2014).
[29]M. Bauchy and M. Micoulaut, J. Non-Cryst. Solids **357**, 2530 (2011).
[30]M. J. Abdolhosseini Qomi, K. J. Krakowiak, M. Bauchy, K. L. Stewart, R. Shahsavari, D. Jagannathan, D. B. Brommer, A. Baronnet, M. J. Buehler, S. Yip, F. J. Ulm, K. J. Van Vliet, and R. J. M. Pellenq, Nat. Commun. **5**, 4960 (2014).